A

Thesis

On

CFD Modeling and Optimization of Magneto-rheological Abrasive Flow Finishing (MRAFF) Process

Submitted by

Soumyajit Das

In partial fulfilment for the award of the Degree of

Master of Technology in **Mechanical Engineering**

Roll No. 213ME2402

Under the Supervision of

Prof.K.P.Maity

DEPARTMENT OF MECHANICAL ENGINEERING

NATIONAL INSTITUTE OF TECHNOLOGY ROURKELA

May, 2015

CERTIFICATE

This is to certify that the project report entitled, **"CFD Modeling and Optimization of Magneto-rheological Abrasive Flow Finishing (MRAFF) Process"** submitted by **Soumyajit Das** in fulfillment for the requirements for the award of Master of Technology Degree in Mechanical Engineering at National Institute of Technology, Rourkela is an authentic work carried out by him under my supervision and guidance. To the best of my knowledge, the matter embodied in the thesis has not been submitted to any other University / Institute for the award of any Degree or Diploma.

Date:

Place:

Prof.K.P.Maity
Dept. of Mechanical Engineering
National Institute of Technology, Rourkela

ACKNOWLEDGEMENT

I feel immense pleasure and privilege to express my deep sense of gratitude, indebtedness and thankfulness to my guide Prof K.P. Maity, Mechanical Engineering Department, National Institute of Technology Rourkela for his invaluable guidance, kind co-operation, inspiration and encouragement in successful completion of the project work.

In this respect I would also like to thank all the faculties and support staff of Department of Mechanical Engineering, NIT Rourkela for providing me all the facilities for my project study and offering their helping hands.

I also convey my heartiest blossoms and thanks to my friends Deeprodyuti Sen, Akash Mukherjee, Shyam Sundar Luha, Vaibhab Agnihotri, Snehasis Biswas for helping me throughout the project work.

At last, I would like to thank my parents for their constant inspiration, encouragement and blessings without which I could not have made this project a success.

Date -

Soumyajit Das

Roll No. 213ME2402

ABSTRACT

A modern nano finishing technique called magnetorheological abrasive flow finishing (MRAFF), which is simply a combined hybrid form of abrasive flow machining (AFM) process and magnetorheological finishing (MRF) process, has been designed for micro finishing of parts even with difficult geometry for a broad range of industrial purposes. In the present work, a model for the prediction of removal of material and surface roughness has been estimated. An effort has been made to study the flow passing through the stainless steel workpiece by CFD modeling in ANSYS 15.0 FLUENT. By assuming the medium as Bingham plastic various parameters affecting the surface roughness has been calculated. Also a theoretical calculation is made for the model if no magnetic field is applied and then comparative study of the two models is proposed. An optimization of the process has also been carried out. With the help of SN Ratio plot and Means plot optimized value of input parameters has been found out to achieve better surface finish.

Keywords: Magnetorheological, MRF, MRAFF, CFD, SN Ratio

CONTENTS

LIST OF FIGURES

LIST OF TABLES

Chapter 1 INTRODUCTION

1.1 Preamble

The available advanced and traditional concluding processes alone are incompetent of producing anticipated surface characteristics on complex geometries and in exercising in-process control on ultimate action. Precision finishing of complex geometries and internal surfaces is always of anxiety being labor intensive and challenging to control. In the contemporary technological world numerous products need a surface roughness of the order of a nanometer (10^{-9} m). It is preferable to use automate the technique where the desired surface finish can be achieved as a function of time. To obtain desired geometrical precision and surface characteristics by removal of unwanted superfluous material from the workpiece surface, small multiple cutting edges of abrasives are usually used. All traditional finishing routes *viz.* lapping, grinding, honing, etc. work on this mechanism of finishing.

Developments in cutting-edge finishing technique in the last few decades have overcome to the relaxation of limitations of tool hardness requirement. The major limitation in final complex geometries is the predefined relative motion of the cutting edge *w.r.t.* the work-pieces surface. The multiple cutting edges in some lightly bonded from are directed to monitor the complex geometries to be finished, is used to overcome this problems. But due to the lack of proper control on the forces, sometime surface and subsurface damages occurs for finishing complex geometry. Numerous advanced finishing techniques have been established to tackle these matters. For example Magnetorheological fluid supported finishing techniques are one such kind of finishing processes, which provides better flexibility towards process control and one can finish with close tolerances. Abrasive flow machine (AFM) [1] is capable of finishing any complex geometry by extruding abrasive-laden polymeric medium through the passage formed by the work-piece and fixture assembly. Controlling the rheological properties of the polymeric by external means is very difficult. Magnetorheological finishing (MRF) [2] is one of the best technique used for external finishing because of the ability to control the acting forces by external means (i.e. magnetic force). By this technique, nanometer level precision can be obtained and it is used commercially to finish optical lenses to the nanometer level. Therefore, a

new precision finishing process, magneto-rheological abrasive flow finishing (MRAFF) has been developed which comprising AFM and MRF for nano-finishing of parts even with complex geometries [3].

1.2 Overview of Magnetorhelogical and Allied Finishing Processes

The available traditional processes are unable of producing desired nano/micro level finishing also these require high expensive equipment, more time consuming and economically incompetent. Magnetorheological Abrasive flow finishing is one of the processes with wide range of application. Before going into the detail discussion of MRAFF process let first discuss other processes i.e. MAF [4], MRF and MFP [5] were the control of performance is done by the use of magnetic field. In these processes, the force acting on the work piece surface through the abrasive particles is controlled externally by changing the magnetic flux density.

1.2.1 Magnetic Abrasive Finishing (MAF)

In this technique, basically ferromagnetic particles are sintered with fine abrasive grains (Al_2O_3, SiC, CBN, or diamond), and those particles are known as ferromagnetic abrasive particles (or magnetic abrasive particles). Fig. 1.1 shows a schematic figure of a plane MAF technique which has the power to control the finishing process is by controlling the application of magnetic field across the machining gap among the top surface of workpiece material and bottom surface of the electromagnet pole which is rotating.

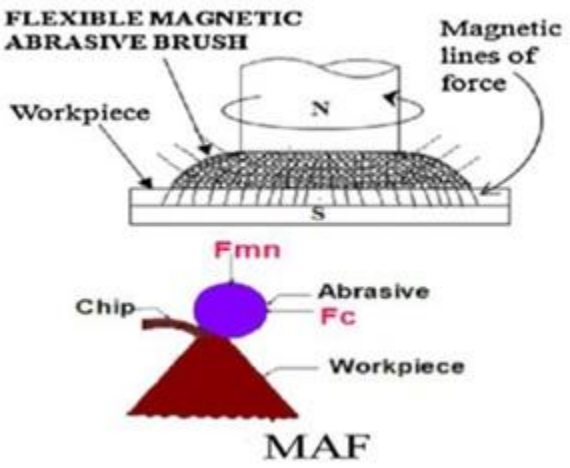

Fig. 1.1 Magnetic abrasive flow machining [6]

1.2.2 Magneto-Rheological Finishing (MRF)

Centre of Optics Manufacturing at Rochester, has designed a process to automate the lens polishing process known as Magnetorheological Finishing (MRF), which relies on a unique ‘‘smart fluid,’’ known as Magnetorheological (MR) fluid. Magnetorheological fluids are suspensions of nano-sized magnetizable grains such as carbonyl iron particles (CIP), dispersed in a non-magnetic carrier medium such as mineral oil or water. When no magnetic field is applied, an ideal magnetorheological fluid shows Newtonian characteristics. Magnetorheological effect is seen when external magnetic field is applied to the magnetorheological fluid. This process is used for finishing optical glasses, glass ceramics and some non-magnetic metals.

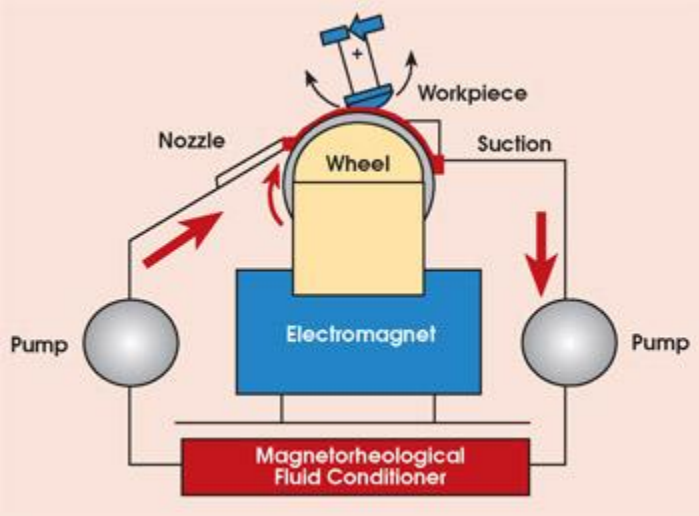

Fig. 1.2 Magnetic Rheological finishing [6]

1.2.3 Magneto Float Polishing

Polishing of spherical surfaces is evenly necessary for which the other two discussed techniques do not meet the criteria. The Magnetic Float Polishing technique has been designed to meet this goals. This process is based on the ferro-hydrodynamic [7] characteristics of magnetic fluid that levitates a non-magnetic float and suspended abrasive particles in it when a magnetic field is applied. The levitation force applied by the abrasives is proportional to the magnetic field gradient which is extremely less and very much adjustable. Magneto float polishing can be a very economic and justified method for nano finishing of brittle materials with spherical and flat shapes. A bank of electromagnets is placed under the finishing chamber [8].

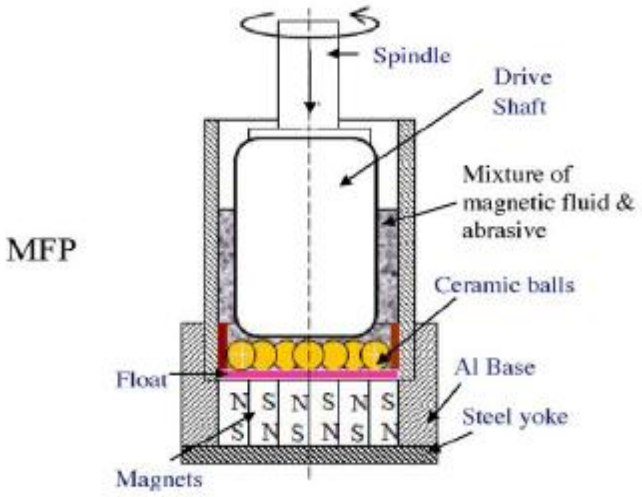

Fig. 1.3 Magneto rheological flow polishing [6]

1.3 Magneto-rheological Abrasive Flow Finishing Process

The process of MRAFF consists of a slug that is magnetized and stiffed with MRP fluid and is flow into and fro through the work piece formed passage. The process of abrasion happens only when a magnetic field is applied on the workpiece, while the other areas are getting unaltered. Fig. 1.4a shows the process. The rheological action of polishing changes with the change in the behavior of the fluid from Bingham to Newtonian plastic and the reverse can also occur when entering and exiting the zone of finishing, (Fig. 1.4b).

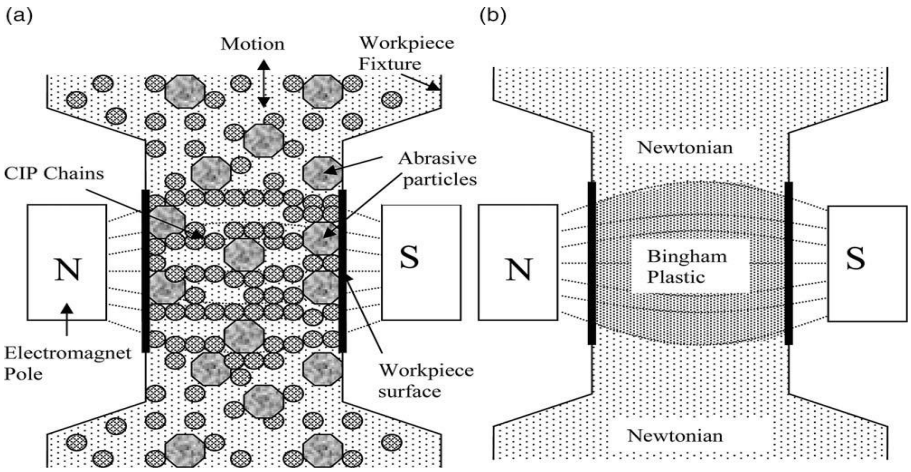

Fig. 1.4(a) MR-abrasive flow finishing mechanism; (b) Change in rheological behaviour of MR-polishing fluid during finishing [3]

The edges of cutting (abrasive cut) held by iron chains of carbonyl rubs the surface of the workpiece and the peaks are thereby sheared from it. The quantity of material that is sheared from the workpiece surface peaks by abrasive grains depends upon the strength which is exhibited by the field-induced structure of MR-polishing fluid and the pressure that has been applied end to end of the piston. This is how the strength of the magnetic field has a control over the degree of abrasion of peaks.

In the process of MRAFF, MRPF is passed through the passage of the workpiece that has to finish applying two cylinders that are opposed by a magnetic field applied externally. The smart magnetorheological viscosity of the fluid (MRPF) that will polish the surface is dependent on the magnetic field strength and the required characteristics of finishing. The Bingham plastic fluid used for polishing shears in an area neighboring the surface of the workpiece. This also enhances removal of the material at a higher rate and thus affects the finishing process. The MRP-fluid extruded through the end to end hollow connection that has been formed on the fixture of the workpiece has been achieved by running two pistons in MRPF cylinders that are opposed using pressure actuators by hydraulic mode.

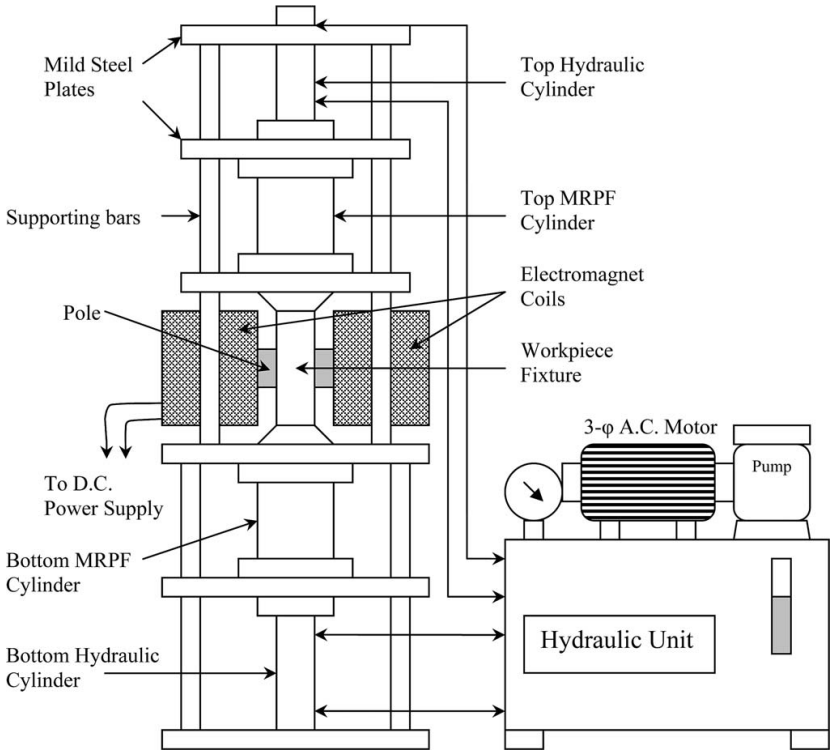

Fig. 1.5 Schematic diagram of the MRAFF setup [3]

The MRAFF setup Fig. 1.5, consists of MRPF cylinders with pistons, workpiece fixture, electromagnet, hydraulic drive and controls, and supporting frame [3].

1.4 Magnetorheological polishing (MRP) fluid

Rabinow [9] invented the magnetorheological (MR) fluid at the end of the 1940-50 decade. They are considered as part of the distinguished controllable materials. The rheological properties of these smart materials can be externally modified by the applying some field of energy. Magneto-rheological-fluids are sols of magnetized particles *viz.*, carbonyl iron, in a non-magnetic emulsion carrier medium *viz.*, oil of silicone, or other mineral or water. The nonappearance of magnetic field causes an ideal magnetorheological-fluid to display Newtonian behavior and on the applying a magnetic field externally, the fluid shows an MR-effect. When we apply a magnetic field, the particles exhibiting magnetic properties inside a non-magnetic fluid carrier accomplish dipole moments that are directly dependent on the field of magnetic strength. The particles that tend to exhibit magnetic properties accumulate into links of dipole moments that are assigned to the direction of the applied field when the dipolar interface in between the particles surpasses their thermal limit of energy. Since energy is absorbed to deform and break these chains, the change in the microstructure is accountable for the commencement of the large finite stress due to the yield that is also controllable. When the fluid is deformed under stress, the chains tend to distort in the direction of applied strain and break when the stresses that are applied go beyond their yield stress induced by field [10]. The particles again rearrange in their random state and the fluid displays their real Newtonian behavior as the field externally applied is removed. When the stress applied onto the linked structure of the magnetorheological-fluid within the existence of field applied, they are modeled as plastic fluid exhibiting Bingham characteristics with the dependence of field with yield stress [11] that can be explained mathematically by the following:

$$\tau = \tau_0(H) + \eta\dot{\gamma} \quad (1)$$

$$\tau = 0 \quad \text{for } \tau<\tau_0 \quad (2)$$

where τ is the shear stress that has been applied, $\dot{\gamma}$ is the rate of shear, η is the dynamic viscosity found from the composition of the base fluid and the magnetic field-induced shear stress. As a result, it depends significantly on the strength of the applied magnetic field, H. The fluid strength

is enhanced when the magnetic field applied is increased. However, the enhancement is not linear in behavior as the particles behave ferro-magnetically and the degree of magnetization at different locations of particle take place in a non-uniform manner [12]. Magneto-rheological fluids conventionally display a yield strength of 50–100 kPa (dynamic) under the influence of a magnetic field of strength 150–250 kA/m [13].The ultimate strength of magneto-rheological-fluid is restricted by the saturation of magnetic influence. The flexibility to electrically modify the rheological behavior of the magneto-rheological-fluid attracts a wide consideration from a varied class of industries as well as multiple applications are too explored. MRP fluid consists of magneto-rheological-fluid having abrasive particles with finer dimensions and dispersed as grains. After applying a magnetic field, the carbonyl iron particles (CIPs) form a continuous link-like structure having columnar assembly and the abrasives being implanted in between. The magneto-force that acts in between the iron grains surrounding abrasive particles provides a bond-strength to it. The scale of the force is dependent on the concentration of iron, applied field intensity of the magnet, magnetic permeability of grains and the particle size.

Chapter 2 LITERATURE REVIEWS

Magnetorhelogical abrasive flow finishing is a microfinishing process on which several research study have been done in the form of research papers, book chapters and patents. A brief review of same has been presented in this section.

Jha and Jain (2004) proposed a structure for CIP chain and surface roughness assessment model. Experiments were done on work piece of stainless steel for different combinations of SiC and CIP particles in magneto-rheological polishing fluid for equal volume concentration. Finishing surface roughness of preliminary profile data and given surface roughness model has also been computer-generated for all combinations of CIP and SiC sizes.

Jha and Jain (2006) describe the effect of magnetic field and no. of cycles on surface roughness and the role of rheological behavior. An experimental setup which is hydraulically powered is designed to understand the process parameters and performance. All the experiments were done on stainless steel material at magnetic field of different strength to examine its outcome on ultimate surface finish.

Das et al.(2008) analysed the bingham plastic medium flow by FEM. Microstructure of the mixture of abrasive particles and ferromagnetic suspended in the MR polishing fluid has been anticipated. A model has also proposed for determining the material removal rate and surface roughness.

Jha et al.discussed the effect on change in the surface roughness of the stainless steel made workpiece due to change in extrusion number of finishing cycles and pressure. Experiments are conducted on a hydraulically powered magneto-rheological flow finishing setup and proposed a new observation named as “illusive polishing” with the result also shows the improvement with increasing of finishing cycles number.

Das et al. (2010)proposed aprocess called Rotational (R)-Magnetorheological Abrasive Flow Finishing procedure as a new polishing technique by creating a rotation on the applied magnetic field which is acting on the MR polishing medium with that to the reciprocating movement resulting from the hydraulic powered unit to smoothen the internal face of cylindrical workpiece made of stainless steel which is in nature a non-magnetic. ANOVA is also conducted and it

confirms that rotational speed of the provided magnet has the highest significant outcome on % improvement in finishing of surface.

Saraswathamma gives a complete literature study of MRF process in case of rheological characterization and experimental analysis, of MR fluid.

Kordonski and Jacobs developed a model that predicts a material removal distribution over the part surface which is in qualitative agreement with experiment on glass.

Kordonski and Golini founds that the energy required for removal of material is supplied by the hydrodynamic flow of Magneto-rheological fluid during a predetermined converging gap created by the surface of the workpiece and a moving stiff wall. It is also found that this finishing process minimizes the surface roughness of optical materials to $\leq 10A^0$.

Cheng et al. investigated the parameters affecting magnetorheological finishing process for example the characteristics of magnetic elements and the distribution of magnetic field. Function of material removal and rate of removal relating a K9 glass mirror is designed and the experiments are explored.

Seoka et al. proposed a fabrication technique on micro-structures of silicon-based curved surfaces with the help of MR finishing process. The most significant factor is getting out as the edge effect. The outcome of magnetic field in the periphery of tool assembly on profiles of finished surface is investigated using a finite element method (FEM). To forecast the profile and curved surface roughness of the workpiece RSM is applied.

Kim et al. highlights the mechanism of material removal of BK7 suspended indifferent slurry conditions for polishing and to examine different surface characteristics, as well as shape analysis study and measurement of improvement in surface roughness, of the portions found out from the magneto-rheological polishing technique with alumina as abrasive particle.

Schinhaerl et al. proposed a mathematical model on magnetorheological finishing process to estimate the polishing tool parameters and it is validated experimentally. It also forecasts the shape and size of an control function and describes the evaluation and distribution of material removal inside the influence function.

Sidpara and Jain (2012) proposed a theoretical model fornormal forces and tangential forces which aredoing the action on the workpiece surface. A squeeze force model for both the forces is also given based on the rolling process theory. It examines that tangential and normal forces increase with increasing concentration of carbonyl iron particle (CIP); though, the value of forces decreases with increasing the concentration of abrasive particles after 3.5%.

Sidpara and Jain (2013) proposed a model to improve the relation of theabrasive-workpiece interaction in the MR fluid based finishing processes. Reduction of forces dominantly seen with the increasing in the angle of curvature of the workpiece exterior because of decrease contact area of workpiece surface andof the magneto-rheological fluid brush.

Singh and Shan proposed thatif a magnetic field is applied in the periphery of the workpiece in abrasive flow machining then there will be a possibility of improvement in the material removal rate and surface roughness. A new set-up has also been designed for magneto abrasive flow machining (MAFM), and it is also studied that how main input parameters are affecting the performance of the technique. Relationships are proposedamong the percentage improvement in surface roughness and the material removal rateof components made with brass. Results obtained from the experiments shows slightly improved performance.

Hua et al. studied the tribological characteristics of MR fluid under a magnetic field. It is seen that wear scar diameter reduces compared to lubrication when no magnetic field is applied. The coefficient of friction rises linearly with the magnetic field, while it reduces as the magnetic field strength weakens.

Niranjan et al. presented amodelfor finishing workpiece exterior in nano range and achieved a surface without defect using MRPF with the help of ball end MR finishing tool. Percentage reduction in surface roughness was determined and compared with that obtained from finishing the workpiece with the help of existing monodispersed MRPF.

Kordonski and Gorodkin proposed a theory about removal of material based on therule of conversation of momentum of particles suspended in a binary system. It is also used to determine material removal in MRF process.

Objectives of Present Work

Based on the literature review it can be said that there is no work has been done in the field of CFD modeling of magnetorheological flow finishing process. The main objectives of the study is as follows -

- To develop a CFD simulation of MRAFF process using ANSYS FLUENT taking stainless steel as work-piece material in a viscoplastic base medium with CIP and abrasive particles suspended in it.
- To determine material removal rate, depth of indentation, axial stress and radial stress and corresponding all the forces to determine the criteria for removal of material and to calculate the surface roughness
- To do a comparative study of magnetorheological abrasive flow finishing process in presence of magnetic field and in absence of magnetic field.
- To determine optimum process parameter for minimization the depth of indentation, axial stress and radial stress so to achieve the better surface finish.

Chapter 3 SIMULATION OF MRAFF

CFD is a computational technique used in engineering to analyze complex real life problems. CFD uses numerical discitization techniques to obtain approximate solutions. The exsactness of the obtained approximate solution depend on the no. of discritization of the phisical domain and the truncation accuracy used for solving the problem.CFD has become feasible due to the advent of high speed digital computers. CFD uses continuum mechanics, hence solves an system of coupled differential equation numerically.

3.1 Advantages of CFD over experiments

The benifits of CFD over experiments are discussed below –

- CFD simulation experiments can be conduct complex problems which may be difficult or outright immposible to achive experimentally. Also, hazards involving the experimentation is avoided.
- CFD is a nondistructive test so it's a very cost effective method. In many problems, such as optimization, fine tuening of many parameters is required. To study such problems experimentally it be required to model prototypes for each parametric optimization carried out. So cost of such eperiment will rise exponentially. Hence, it is always advisible to opt for CFD based solution.
- Simulation-based design instead of "build & test".CFD provides high-fidelity database for diagnosing flow field.CFD provides exact and detailed information about HVAC design parameters: CFD gives broader and more detailed information about the flow within an occupied zone, and meets this goal better than any other method.
- CFD is more consistent because the simulation schemes and methods upon which CFD is based are improving rapidly. Also using normal programming software such as C, frotron and matlab it is posible to design solver based on the complex physics associated with the problem hence yielding a more real life solution. Final experimental testing of an approved CFD model can be conducted to check for its consistency.

3.2 Application of CFD

For the benefits discussed above now a days it has seen that CFD is been used in various fields. Some of the area discussed here -

- **In validation/optimization of HVAC design parameters**
  CFD analysis is done to validate many design aspects such as exhaust temperature , flow rate, location and no. of diffuser and exhausts.So it is seen that all the design criteria can be finely tuned using CFD analysis
- **In modification/improvement of malfunctioning HVAC systems:**
  With the use of robust CFD solver, it is possibe to get solution depending on application. Also fault analysis of the system under study can be achived hecnce, dectecting malfuntions.
- **In comparisons between alternative systems:**
  For cirtain design layout, there exsists severa methodology for designing HVAC systems for a space. As stated earier, CFD application can improve design and also be able in comparing different design, thus yielding a better altenative system.
- **In an engineering investigation:**
  CFD analysis of of many control variable such as pressure, temperature chemical concentration gives new insigh in understanding complex procedures. It also helps engineers and scientist make proper decision [14].

3.3 Modeling

Modeling is the art of converting a physical problem into the language of mathematics. In doing so many assumtions are made reducing the complexity of the problem. But, it is very important to preserv the basic physics of the problem while appling the assumption as it my lead to very unrealistic solutions. Modelling includes:

3.3.1 Geometry and domain–Domain of the problem is bsically defined as the space over which the solution is opted for. The domain may be a complicated in geometry. Classic approaches of the above process are as follows –

- Geometry approximation
- CAD/CAE integration: use of industry standards such as SOLID WORKS, ACIS, CATIA, IGES,PRoE etc.
- The three coordinates: Choice of coordinate system depends on the symmetry of the problem. Choosing appropiate coordinate system yields is less complecated equations, hence leading to less computational time.

3.3.2 Coordinates – Thenumerical solution for a given flow depends on the coordinates (grid) used to compute the flow. Three types of coordinates are used as cartesian,cylindrical and spherical.

3.3.3 Governing equations – There are few basic equation of continuity and momentum are used for the analysis of the problem. Some of them are –

- Continuity equation

$$\frac{\partial \rho}{\partial t}+\frac{\partial(\rho u)}{\partial x}+\frac{\partial(\rho v)}{\partial y}+\frac{\partial(\rho w)}{\partial z}=0 \tag{3}$$

- Navier-Stokes equations (3D in Cartesian coordinates)

$$\rho\frac{\partial u}{\partial t}+\rho u\frac{\partial u}{\partial x}+\rho v\frac{\partial u}{\partial y}+\rho w\frac{\partial u}{\partial z}=-\frac{\partial \hat{p}}{\partial x}+\mu\left[\frac{\partial^2 u}{\partial x^2}+\frac{\partial^2 u}{\partial y^2}+\frac{\partial^2 u}{\partial z^2}\right] \tag{4}$$

$$\rho\frac{\partial v}{\partial t}+\rho u\frac{\partial v}{\partial x}+\rho v\frac{\partial v}{\partial y}+\rho w\frac{\partial v}{\partial z}=-\frac{\partial \hat{p}}{\partial y}+\mu\left[\frac{\partial^2 v}{\partial x^2}+\frac{\partial^2 v}{\partial y^2}+\frac{\partial^2 v}{\partial z^2}\right] \tag{5}$$

$$\rho\frac{\partial w}{\partial t}+\rho u\frac{\partial w}{\partial x}+\rho v\frac{\partial w}{\partial y}+\rho w\frac{\partial w}{\partial z}=-\frac{\partial \hat{p}}{\partial z}+\mu\left[\frac{\partial^2 w}{\partial x^2}+\frac{\partial^2 w}{\partial y^2}+\frac{\partial^2 w}{\partial z^2}\right] \tag{6}$$

3.3.4 Flow conditions - Based on the many physical phenomenon that a fluid flow may be characterized in, CFD solver can be distinguished into different catagories:

- Viscous vs. inviscid depending Renolds no.(Re)
- External flow and/or internal flow (wall bounded or not)
- Turbulent or laminar reliant on Renolds no.(Re)
- Incompressible vs. compressible depending on Mach no. (Ma)

- Single- vs. multi-phase, where phase chane may occur during the process (Ca)
- Thermal/density effects (includs effect of natural and/or forced convection Pr, g, Gr, Ec)
- Free-surface flow (Fr) and surface tension (We)
- Chemical reactions and combustion (Pe, Da) [15]

3.3.5 Initial and boundary conditions –Intial conditions for steady and unsteady flow can be classified as -

- ICs generally affects the convergence path rather than the final solution.
- ICs should be reasonable enough such that solution path must be convergent.
- Better initial conditions are obtained for complex unsteady CFD problem by running the steady part for a couple of times

For BCs certain assumtion are taken such as no-slip or/and slip-free on walls, periodic, outlet (perpetual pressure, rapidity convective, algebraic beach, zero-gradient), and non-reflecting (for density varient flows, such as sound studies), etc.

3.4 How does CFD work

CFD packages comprise sophisticated user boundaries inputproblem parameters and to inspect the results.Hence all codes comprise three main elements -

1. Pre-processor

2. Solver

3. Post - processor

3.4.1Pre-Processor

Pre-processor consists of the input of a flow problem to a CFD program by means of an operator-friendly interface and the subsequent transformation of this input into a form suitable for use by the solver. Pre processing stage involves fixing the domain, Generation of grids, Selection of physical and chemical phenomena, Definition of fluid properties, and Specification of appropriate boundary conditions. Following are the user activities –

- define geometry & generate grid
- selection of phenomena to be modeled
- definition of fluid properties
- specification of boundary and initial conditions

3.4.2 Solver

Three primary numerical solution techniquesfinite difference, finite element and finite control volume. In outline the numerical methods that form the basis of solver. The numerical method done by the following:

- Approximates the unknown variables by simple functions
- Discretization by substitution of the approx-imations into the governing flow equations and subsequent mathematical manipulations
- Solution of the algebraic equations

3.4.2.1 Finite volume method (FVM)

Based on control volume formulation of analytical fluidsThe domain is divided into a number of control volumes (aka cells, elements) - the variable of interest is located at the centroid of the control volume. The differential form of the governing equations are integrated over each control volume. Finite difference approximations are substituted for the terms in the integrated equations (discretization) converts the integral equations into a system of algebraic equations.Set of algebraic equations are solved by an iterative method.

$$\frac{\partial}{\partial t}\iiint Q dv + \iint F dA = 0 \tag{7}$$

where Q - vector of conserved variables

F - vector of fluxes

V - cell volume

A - Cell surface area

3.4.2.2 Finite element method (FEM)

The finite volume method (FVM) represents an efficient and robust method forthe solution of inviscid compressible flow. On the other hand, it is well-knownthat the finite element method (FEM) is suitable for the approximation of ellipticor parabolic problems. It is mainly is appliedto the approximation of viscous terms.

$$R_i = \iiint W_i Q dv^e \tag{8}$$

R_i - Equation residual at an element vertex

Q - Conservation equation expressed on element basis

W_i - Weight Factor

3.4.2.3 Finite difference method (FDM)

Finite difference methods describe the unknowns ϕ of the flow problems by means of point samples at the node points of a grid co-ordinate lines. Truncated Taylor series expan-sions are used to generate finite difference approximations of the derivatives of ϕ in terms of point samples of ϕ at each grid point and its immediate neighbors.

$$\frac{\partial Q}{\partial t} + \frac{\partial F}{\partial x} + \frac{\partial G}{\partial y} + \frac{\partial H}{\partial z} = 0 \tag{9}$$

where, Q - Vector of conserved variables

F,G,H - Fluxes in the x ,y, z directions [16]

3.4.3 Post-Processor

As in pre-processing a huge amount of development work has recently taken place in the post-processing field. Owing to the increased popularity of engineering workstations, many of which have outstanding graphics capabilities, the leading CFD packages are now equipped with versatile data visualization tools. These include –

- Domain geometry and grid display
- Vector Plots
- Contour Plots
- Particle Tracking

3.5 Present Study

In the current study a 2D computational fluid dynamics (CFD)simulation of the medium along the workpiece fixture has been carried out in ANSYS 15 FLUENT to calculate the axial stress, radial stress and depth of indentation to find out the volumetric material removal rate. Also a calculation has been made to find out the surface roughness to examine the level of precision that can be achived by this finishing process.

3.5.1 Govering Equations

The mathematical depiction of the flow of magnetorheological polishing fluid in Magnetorheologial abrasive flow finishing process involves general equations of continuity and momentum. At first the basic equation of continuity and then the z-component of momentum equation in cylindrical coordinate system are solved. For Bingham plastic fluid, relation between viscosity and shear rate ($\mu = f(\dot{\gamma})$) [17] which is a nonlinear function. For the present work, viscosity is not justdepends on shear rate althougha function of the applied magnetic effect through $\tau_{y.}$ Thus, it is a bit difficult to solve the analytical solution of Navier–Stokes equation and therefor CFD simulation is carried out.

Following are the assumptions used tomake simplier the analysis work:

- The medium is taken as homogeneous, isotropic and incompressible in nature.
- The flow is sassumed as a steady and axi-symmetric flow
- A fully developed flow is assumed (i.e. $v_r = 0$, $dv_z/dz = 0$) with no spin ($v_\theta = 0$)
- $\tau_{rz} = \mu(dv_z/dr)$

After applying the above assumptions the final form of the continuity and z-component of the momentum equation is summarised as

$$-\frac{dp}{dz} + \frac{\mu}{r}\frac{dv_z}{dr} + \mu\frac{d^2v_z}{dr^2} + \left(\frac{d\mu}{dr}\right)\left(\frac{dv_z}{dr}\right) + \rho g_z = 0 \quad (10)$$

where v_z and v_r are z and r components of the velocity. $\delta p/\delta z$ is pressure gradient in the z direction and it is obvious to change linearly from inlet to exit of the computational zone, and it is determined as $\delta p/\delta z = -(P_{applied} - P_{friction})/L$. Here, $P_{friction}$ is the loss of pressure because of the piston friction and in the currentstudy it is taken as equivalent to 15 bar. $P_{applied}$here is the pressure applied by the pump and L is taken as the length of fixture. With appropriate boundary conditions Eq. (10) is solved computationally for getting the velocity profile (v_z) and afterward the shear-stress profile at each grid point radially.

3.5.2 Boundary conditions and discretization in CFD

It is necessary to be careful to make sure that the discretization is managing the discontinuous solutions accordingly. The Euler equations and Navier- Stokes equations both admit shocks, and interaction surfaces.

- A uniform velocity profile at inlet and a constant pressure at outlet is maintained with a fully developed flow condition.
- No slip boundary condition is used along the wall.
- An axes of symmetric boundary condition is used along the axes of the cylindrical fixture.
- The inlet pressure is 37.5 bar.

The computational field is discretized radially from grid point i = 1 to N. As Equation (10) is a second order regular differential equation, so to completely describe the problemtwo boundary conditions are needed. They are,

(a) at $r = r_f$, $v_z = 0$

(b) at $r = 0$, $dv_z/dr = 0$

To discretize the Eq. (10) finite-difference method is used.

3.5.3 Geometry of workpiece

In the present study a cylindrical work piece made up of stainless steel is taken with dimension of 35 x 5 x 2 mm^3.

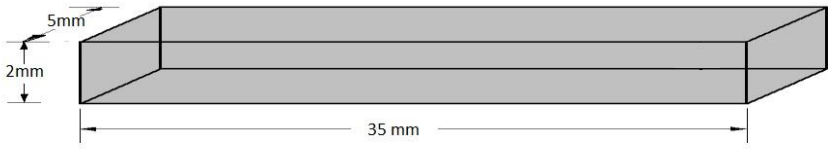

Fig. 3.1 Stainless steel workpiece with dimension

3.5.4 Geometry of workpiece fixture

The workpiece fixture is a cylindrical type of fixture with internal slots on both sides where the workpice to be positioned.

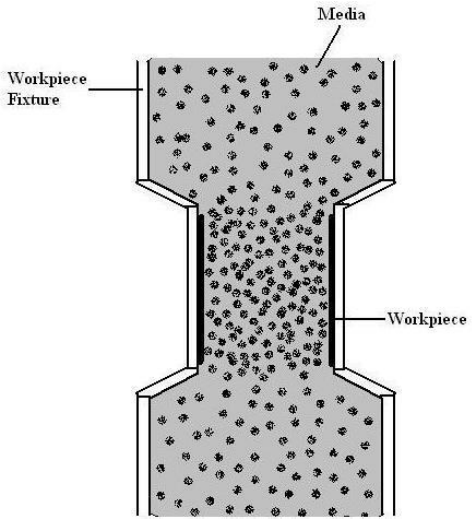

Fig. 3.2 The workpiece fixture [3]

3.5.5 Meshed diagram of workpiece fixture

As this workpiece is symmetric in nature therefore we have created half of the work piecewhich will be automatically rotated in Fluent.

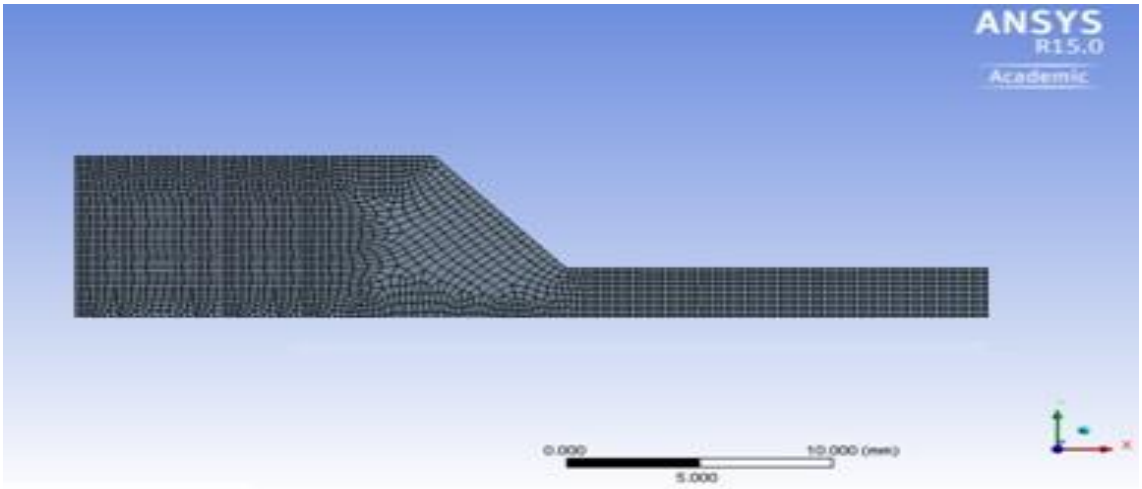

Fig.3.3 Meshed diagram of workpiece with fixture

3.5.6 Parameter setting

Work piece: Stainless steel
Brinnel hardness no: 277 BHN
Ultimate tensile strength: 860 MPa
Yield strength in shear:540.30 MPa

Polishing Fluid: 20% by volume CIP, 20% by volume SiC abrasive of mesh size 800, and 60% by volume of viscoplastic base medium (20wt% AP3 grease and 80 wt% paraffin liquid heavy).

3.5.7 Modelling of material removal

Following are the assumptions taken for the current study of removal of material by Magnetorheolocical abrasive flow finishing process:

- Each and every abrasive grains shapes are assumed to be spherical and of the equal size.Also the average diameter is determined from the total number of mesh size.
- Each grain is assumed to have a one active cutting edge and the pressure applied on everygrain is assumed to be constant and equal to the value of average load.
- It is also assumed that each abrasive particle to achieve the equal penetration depth reliant upon the given average force and the properties of workpiece material.

- Material removal is assumed due to the translation and indentation of abrasive particles each time whwn particle and workpiece interference take place.

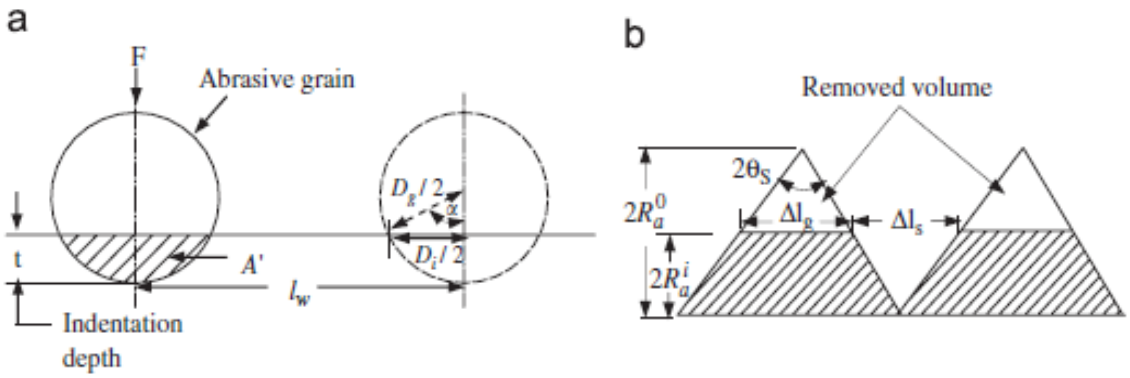

Fig. 3.4(a) Schematic diagram of the indentation of a spherical abrasive grain on the workpiece surface, and (b) shape of the peak of the irregularity machined [17]

The normal force whichisdeveloping from the total magnetic force applied on an abrasive grainis the reason behind the penetration of the workpiece surface. Due to shear force which is generating because of piston movement when the particle is horizontally translated, the plastically destroted zone under the surface gets inclined. It gives rise to upward flow and because of that chip is formed, which is correspondingly sheared from the surface of the workpiece. The Brinell hardness number (BHN) can be interrelated to the depth of indentation in the workpiece surface as follows:

$$BHN = \frac{F_N}{\left(\frac{\pi}{2}\right)D_g\left(D_g - \sqrt{{D_g}^2 - {D_i}^2}\right)} \qquad (11)$$

Where, $F_N = F_m + F_n$ (12)

and, $F_m = (m\chi_m B\nabla B)/\mu_o$ [18] (13)

$F_n = \sigma_{rad} \text{x } A$ (14)

F_m is Indentation force on the workpiece surface, m = mass of CIP, χ_m = mass susceptibility of CIP (m^3/kg), B is magnetic field density = 0.5T,$\nabla B = \delta B/\delta x$, gradient of a magnetic field,assumed here as 1, μ_0= is permeability in free space (4π x 10^{-7}Wb/Am), σ_{rad} is the radial stress acting on

the work piece surface, A is total cross-sectional area of the abrasive particle, D_i is indentation diameter and D_g is the diameter of abrasive particle (19 mm). From Viker's micro-hardness testing machine the hardness of stainless-steel workpiece is found as 277 BHN [19]. The depth of indentation 't' is obtained as

$$t = \frac{D_g}{2} - \frac{1}{2}\sqrt{{D_g}^2 - {D_i}^2} \quad (15)$$

From Fig. 3.4(a), the cross-sectional area A' of the groove generated (shaded portion of the grain) is derived from the following:

$$A' = \frac{D_g^2}{4} \sin^{-1}\frac{2\sqrt{t(D_g - t)}}{D_g} - \sqrt{t(D_g - t)}\left(\frac{D_g}{2} - t\right) \quad (16)$$

The initial surface profile of the workpiece is assumed to be triangular [20] as shown in Fig 3.4(b). It is assumed that initial surface profile of the workpiece is uniformly distributed with initial surface roughness R_a^0 and abrasives move perpendicular to the direction of the scratches. Volume of material removed (Vg) by an abrasive grain is obtained as

$$V_g = A'\left(1 - \frac{R_a^i}{R_a^o}\right)l_w \quad (17)$$

where, l_w is the total length of the workpiece = 35mm, R_a^i is surface roughness after ith cycle. As the total material removal is made up of number of similar cycles, total number of abrasive grains (n_S) indenting into the workpiece surface per stroke is given by

$$n_s = 2\pi r_f N_s l_s \left(\frac{r_c}{r_f}\right)^2 \quad (18)$$

where, l_S is stroke length of the piston = 50mm, N_s is the number of active abrasive particles per unit area of workpiece = 1200, r_c is radius of the medium cylinder = 28.75mm and r_f is radius of the workpiece fixture = 9mm. Volumetric material removal (M_V) in ith stroke is given by

$$M_v = \frac{\left(R_a^0 - R_a^i\right)^2}{R_a^0} l_w^2 \quad (19)$$

Since volumetric material removal (M_v) in ith stroke = volume of material removed by an abrasive grain (V_g) × total number of abrasive grains indenting the workpiece surface per stroke (n_S) [21], and it is given as

$$M_v = 2\pi_f N_s l_s \left(\frac{r_c}{r_f}\right)^2 \left[\frac{D_g^2}{4} sin^{-1}\frac{2\sqrt{t(D_g-t)}}{D_g} - \sqrt{t(D_g-t)}\left(\frac{D_g}{2}-t\right)\right]\left(1-\frac{R_a^i}{R_a^o}\right) l_w \quad (20)$$

Comparing Eq. (19) with Eq. (20), and after simplification we obtain

$$R_a^i = R_a^0 - 2\pi r_f N_s \left(\frac{l_s}{l_w}\right)\left(\frac{r_c}{r_f}\right)^2 \left[\frac{D_g^2}{4} sin^{-1}\frac{2\sqrt{t(D_g-t)}}{D_g} - \sqrt{t(D_g-t)}\left(\frac{D_g}{2}-t\right)\right] \quad (21)$$

Surface roughness for ith cycle is calculated from Eq. (21)

Simulation results of the fluid flow through the workpiece fixture is analyzed. Then calculation is made to find the numerous parameters like total normal force, shear force, indentation depth and material removal from the analysis data.

4.1 Velocity Distribution

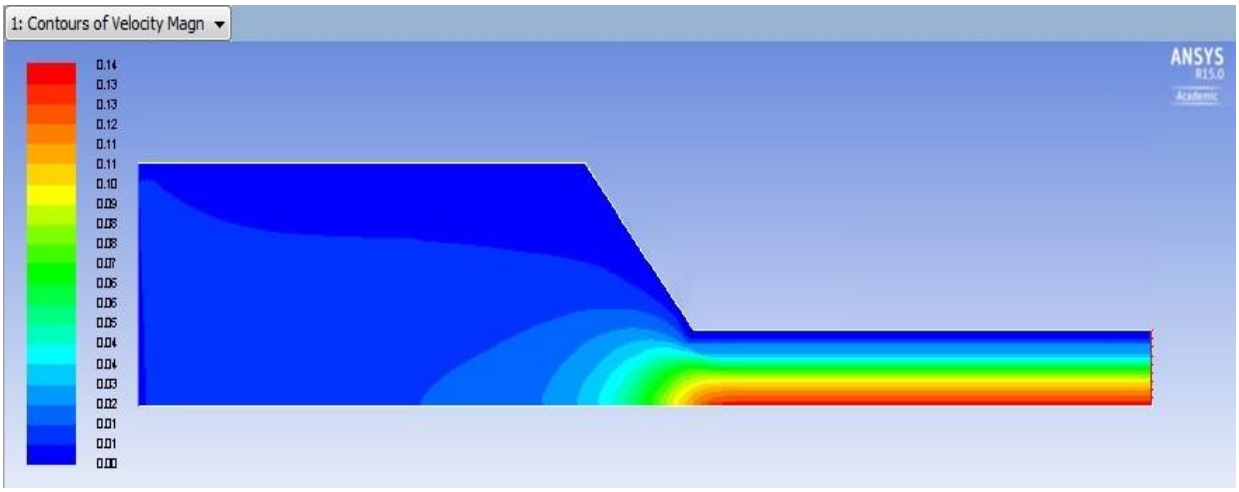

Fig. 4.1 Velocity distribution along the workpiece fixture

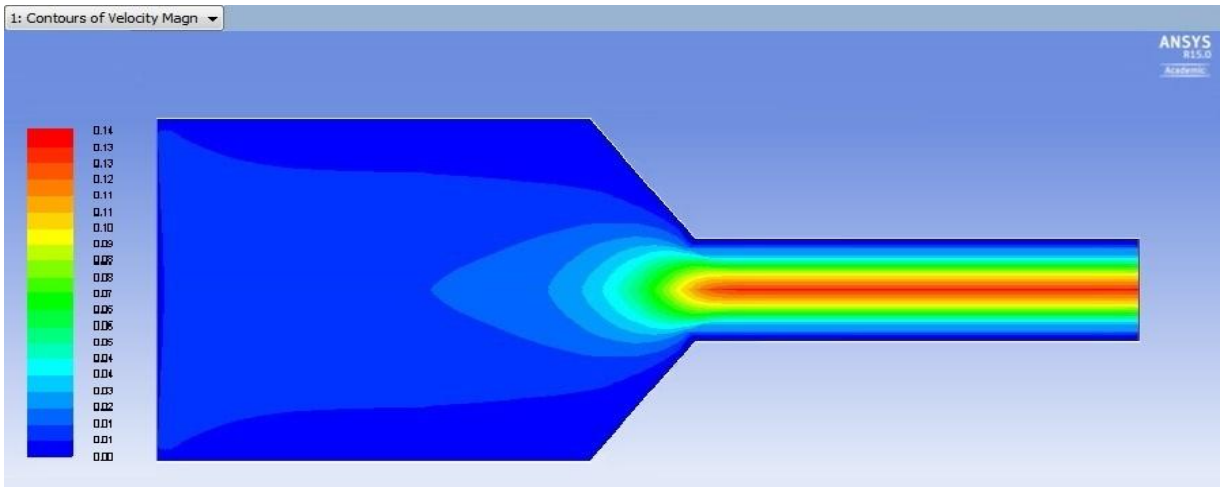

Fig. 4.2 Velocity distribution on full view of work piece fixture

Reference to the Fig. 4.1,4.2 we can conclude that the velocity changes when it reaches the taper exit, magnitude of velocity is maximum at the centre and decreases gradually towards the wall, because the effect of high viscosity present in the media.

4.2 Pressure Distribution

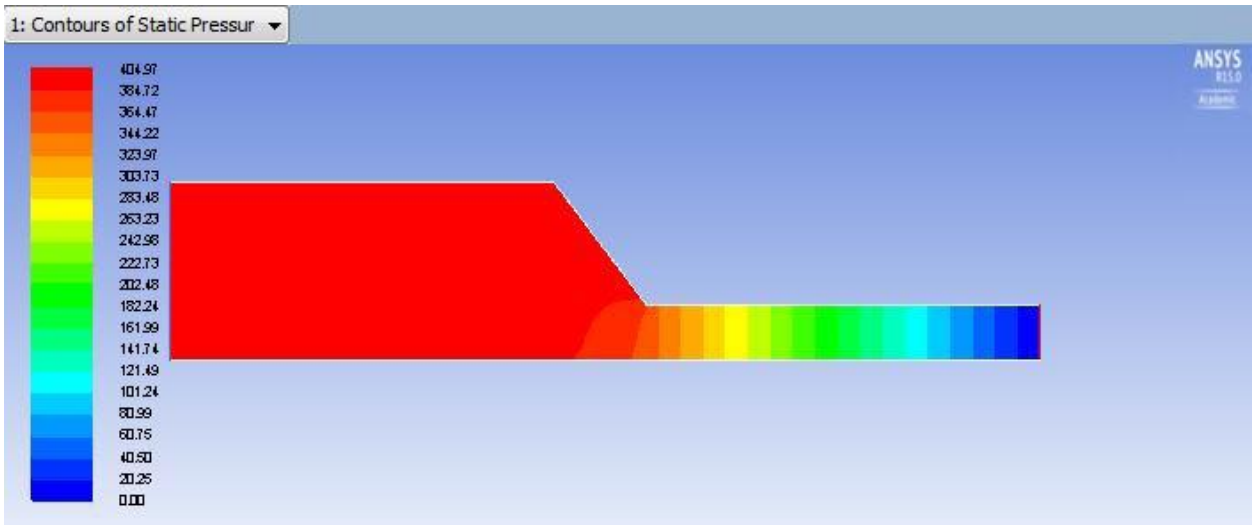

Fig. 4.3Pressure distribution along the workpiece fixture

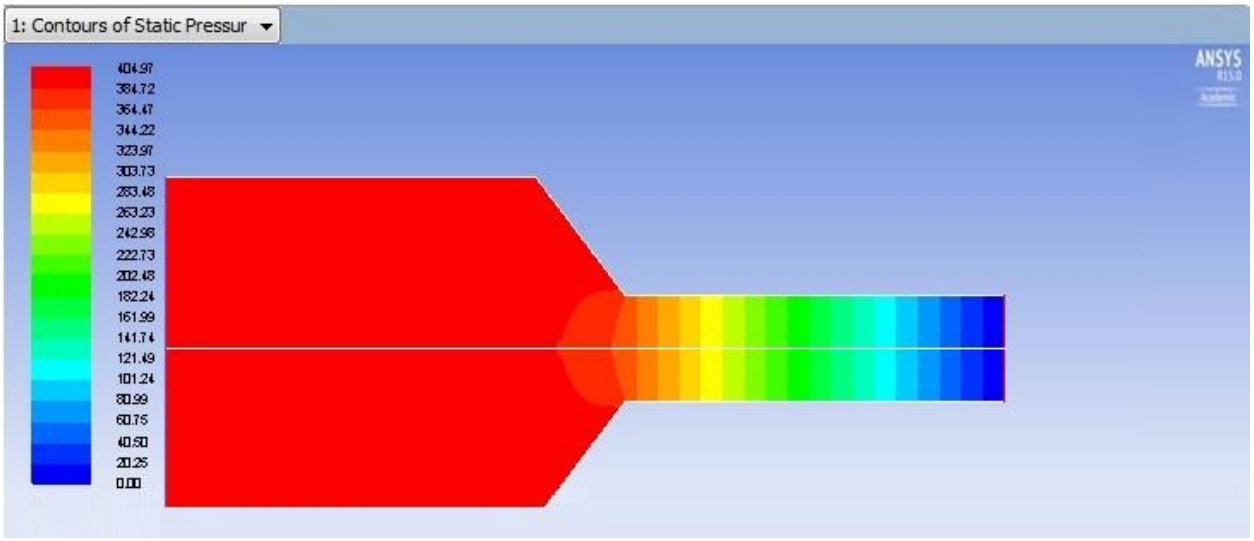

Fig. 4.4Pressure distribution on full view of work piece fixture

Reference to the Fig. 4.3,4.4 it is seen that the pressure distribution in the region of work piece fixture remains constant upto theexit of the taper. After that it decreases gradually to the end of the workpiece.

4.3 Strain Rate Distribution

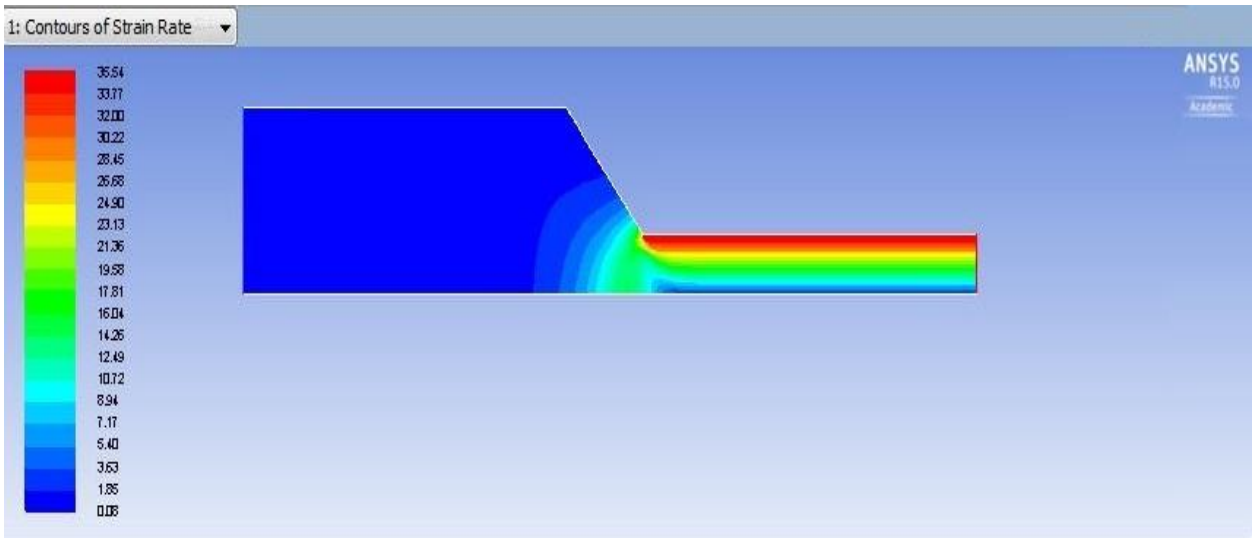

Fig. 4.5Strain distribution along the workpiece fixture

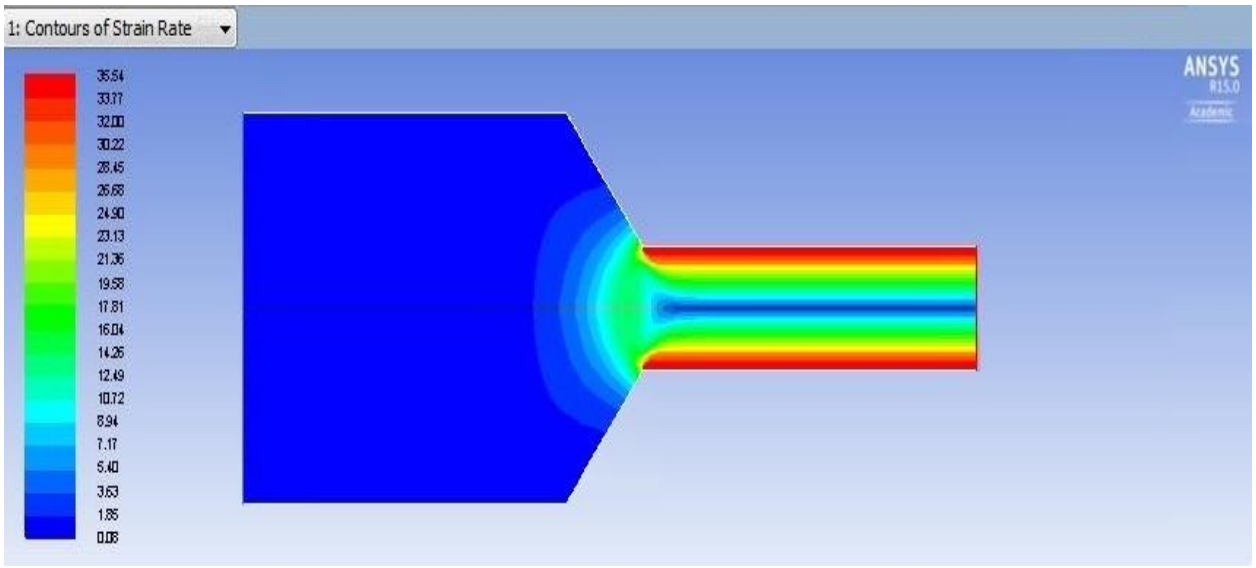

Fig. 4.6 Strain distribution of full view of work piece fixture

Reference to the Fig. 4.5,4.6 we can conclude that the strain is maximum at the wall. That's why stress will be produced there to remove the material.

4.3.1 Plot of axial wall shear stress with position

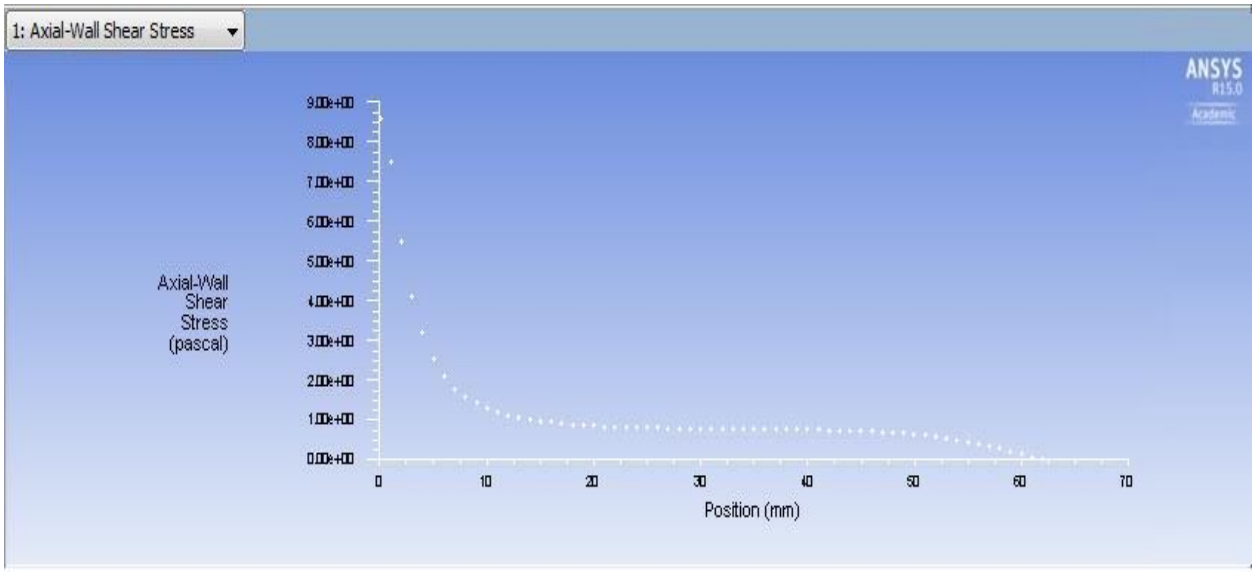

Fig. 4.7 Axial wall shear stress with position

4.3.2 Plot of radial wall shear stress

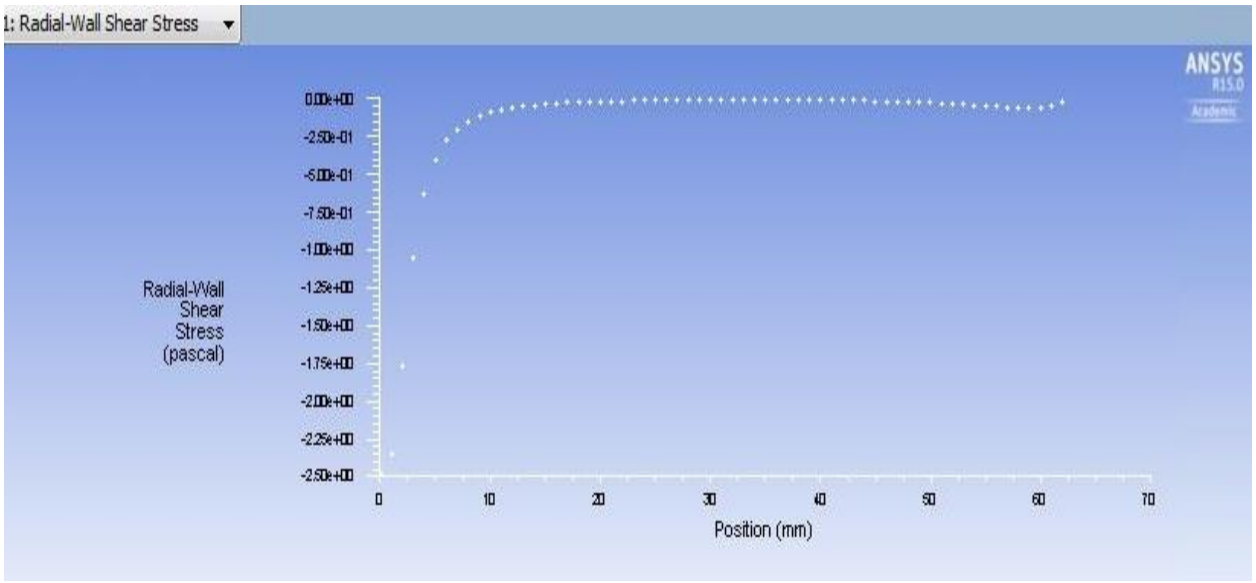

Fig. 4.8Radial wall shear stress with position

Reference to the Fig. 4.7,4.8 the axial and radial stress can be obtained from the graph and are used for furher calculation.

4.3.3 Calculation

From CFD calculation the radial stress on the work piece material it is found as

σ_{rad} = 0.0607106 Pa

So, we got the total indentation force F_N = 4.167 X 10^{-10} N

Now the indentation diameter can be calculated by putting the value of F_N in equation

D_i = 4.106 X 10^{-8} m

Now we get depth of indentation, t = 1.041 X 10^{-10} m

Then projected area can be calculated as,

A' = 3.604 X10^{-20} m^2

Now F_{shear} and F_R are given as,

F_{shear} = (A- A') x shear stress of the field

and F_R= A' x σ_{yps}

where, σ_{yps} = yield point stress of stainless steel workpiece = 540.30 MPa

Now we obtained F_{shear} and F_R as 1.89 x10^{-6} N and 4.71x10^{-11} N.

As we see $F_{shear} > F_R$. So material removal should happen on the workpiece surface.

Surface roughness has also been calculated for 200 cycles (i = 200) and found as 0.43µm.

4.3.4 Validation with Experimental Results

- From previous experimental data [17] it is found that F_{shear} and F_R value is 1.25 x 10^{-5} and 2.76 x 10^{-10} respectively. So we can say that the model is validated.
- Surface roughness has also been calculated for 200 cycles and found as 0.43µm. From previous paper [3] it is seen that R_a value is calculated as 0.34µm. So we can say that the prediction is correct.

4.3.4 A new model when no magnetic field is applied

The calculation is also made for no magnetic effect and then the results are compared with the actual modeling.

As the magnetic effect is neglected. So in the calculation for total normal force F_N ,the magnetic component F_m is omitted and then the corresponding calculation is made without changing the other formulaes.

The value we got as,

$F_N = 3.43 \times 10^{-12}$

$F_{shear} = 4.18 \times 10^{-8}$ and $F_R = 4.71 \times 10^{-11}$.

As we see here $F_{shear} > F_R$. So removal of material should undergo on the workpiece. But as the normal force acting on the abrasive is so less so there is not such improvement in surface finish and surface rouhness found as 0.11 μm.

Chapter 5 OPTIMIZATION

As the main concern is to get high surface finish so it is necessitate to optimizethe process parameters to achieve the requisite level of finishing. There are numerous methods ofoptimization existing. In this paper Taguchi's analysisis applied to find the optimum process parameters.

5.1 Taguchi Design

A Taguchi design is a designed experiment that helps to choose a product or process that functions more constantly in the working environment. Taguchi designs recognize that not all factors that cause variability can be controlled. These uncontrollable factors are called noise factors. Taguchi designs try to identify controllable factors (control factors) that minimize the effect of the noise factors. During experimentation, you manipulate noise factors to force variability to occur and then determine optimal control factor settings that make the process or product robust, or resistant to variation from the noise factors. A process designed with this goal will produce more consistent output. A product designed with this goal will deliver more consistent performance regardless of the environment in which it is used [22].

5.1.1 SN Ratio

In Taguchi designs, a measure of robustness used to identify control factors that reduce variability in a product or process by minimizing the effects of uncontrollable factors (noise factors). Control factors are those design and process parameters that can be controlled. Noise factors cannot be controlled during production or product use, but can be controlled during experimentation. In a Taguchi designed experiment, you manipulate noise factors to force variability to occur and from the results, identify optimal control factor settings that make the process or product robust, or resistant to variation from the noise factors [23]. Higher values of the signal-to-noise ratio (S/N) identify control factor settings that minimize the effects of the noise factors.

Taguchi experiments often use a 2-step optimization process. In step 1 use the signal-to-noise ratio to identify those control factors that reduce variability. In step 2, identify control factors that move the mean to target and have a small or no effect on the signal-to-noise ratio.

The signal-to-noise ratio measures how the response varies relative to the nominal or target value under different noise conditions. You can choose from different signal-to-noise ratios, depending on the goal of your experiment. For static designs, Minitab offers four signal-to-noise ratios:

Table No. 5.1: Signal-to-noise ratios [24]

Signal-to-noise ratio	**Goal of the experiment**	**Data characteristics**	**Signal-to-noise ratio formulas**
Larger is better	Maximize the response	Positive	$S/N = -10 * \log(\Sigma(1/Y^2)/n)$
Nominal is best	Target the response and you want to base the signal-to-noise ratio on standard deviations only	Positive, zero, or negative	$S/N = -10 * \log(\sigma^2)$
Nominal is best (default)	Target the response and you want to base the signal-to-noise ratio on means and standard deviations	Non-negative with an "absolute zero" in which the standard deviation is zero when the mean is zero	$S/N = -10 * \log((\acute{Y}^2)/\sigma^2))$
Smaller is better	Minimize the response	Non-negative with a target value of zero	$S/N = -10 * \log(\Sigma(\acute{Y}^2)/n))$

5.1.2 Means

The mean is the average response for each combination of control factor levels in a static Taguchi design. Depending on the response, your goal is to determine factor levels that either minimize or maximize the mean.

5.2 Result and Discussions

The characteristic parameters of magnetorheological abrasive flow finishing aretaken of 3 variables and their domains are shown in Table no. 5.1 with high,medium and low value. L9 orthogonal array is used. A randomized table for L9 orthogonal array is shown in Table no. 5.2. Design ofExperiment (DOE) [25] of above said three parameters with 9 runs is given in Table no. 5.3. Theinput variables of this machining are taken as magnetic field density, pressure and velocity.The value of output responses i.e. axial stress, indentation depthandradial stress are recorded in Table no. 5.4. Minitab edition 15is utilized for the optimization. It will give us the SN ratio and Mean plots for each output responses from which we can conclude the optimze process parameters.

Table. 5.2 Value of Input Process Parameters

Process parameters	**Unit**	**Code**	**Low (1)**	**Medium (2)**	**High (3)**
Magnetic Field Density	T	A	0.3	0.4	0.5
Pressure	bar	B	30	37.5	45
Velocity	m/sec	C	0.01	0.02	0.03

Table No. 5.3: Randomized Design Table

Run	A (Magnetic Field Density)	B (Pressure)	C (Velocity)
1	1	1	1
2	1	2	2
3	1	3	3
4	2	1	3
5	2	2	1
6	2	3	2
7	3	1	2
8	3	2	3
9	3	3	1

Table No. 5.4: Design table

Run	A (Magnetic Field Density)	B (Pressure)	C (Velocity)
1	0.3	30	0.01
2	0.3	37.5	0.02
3	0.3	45	0.03
4	0.4	30	0.03
5	0.4	37.5	0.01
6	0.4	45	0.02
7	0.5	30	0.02
8	0.5	37.5	0.03
9	0.5	45	0.01

Table No. 5.5: Value of Output Responses

Run Order	Axial Stress	Radial Stress	Indentation Depth
1	31.547	0.144	0.064
2	38.659	0.148	0.084
3	31.215	0.254	0.094
4	37.954	0.084	1.064
5	33.644	0.184	0.073
6	31.789	0.154	0.088
7	41.124	0.104	1.114
8	40.113	0.156	1.140
9	38.455	0.218	1.128

5.2.1 Axial Stress

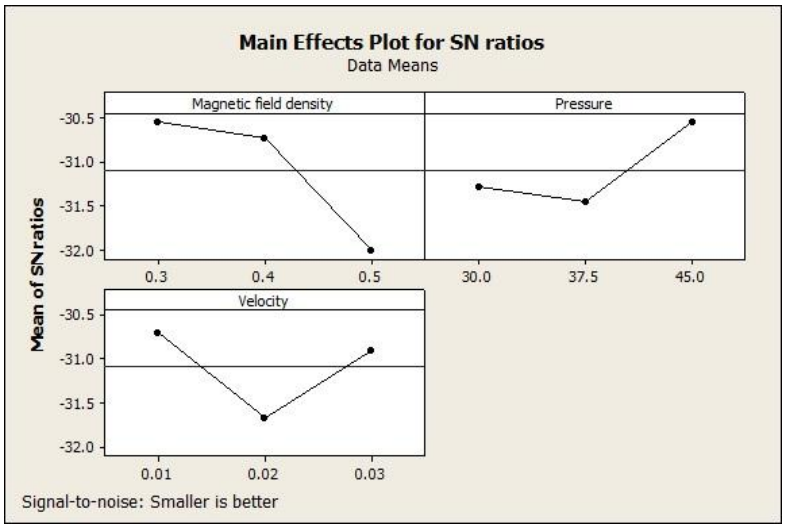

Considering the nano level finishing low axial stress will be justified because then the axial force will be less corresponding to the indentation depth. So here smaller is better criteria is taken. Now it is known that the higher values of SN Ratio will give the optimum input parameters for requirement consideration. So from the plot it can be said that the optimum paramaters for axial stress are 0.3T magnetic field density, 45 bar pressure and 0.01 m/sec velocity.

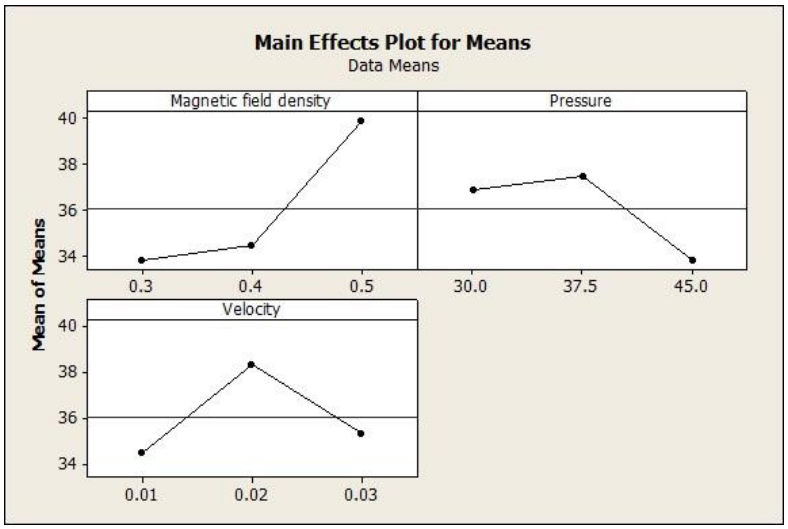

For the Means plot it is known that the lower values will give the optimum input parameters for requirement consideration. So from the plot it can be said that the optimum paramaters for axial stress are 0.3T magnetic field density, 37.5 bar pressure and 0.02 m/sec velocity.

5.2.2 Radial Stress

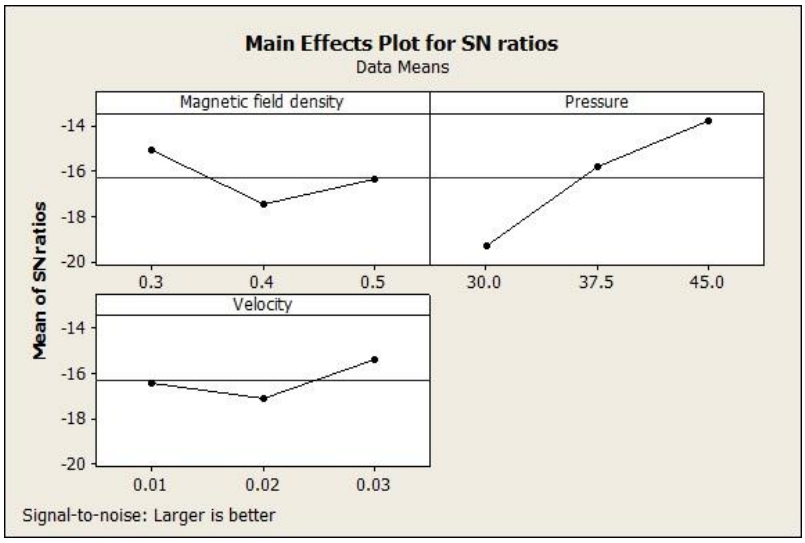

Considering the nano level finishing high radial stress will be justified because to be able to do the material removal it is necessary that shear force should be high. So high value of radial stress is required. That is why here higher is better criteria is taken. Now it is known that for the above criteria higher values of SN Ratio will give the optimum input parameters. So from the plot it can be said that the optimum paramaters for radial stress are 0.3T magnetic field density, 45 bar pressure and 0.03 m/sec velocity.

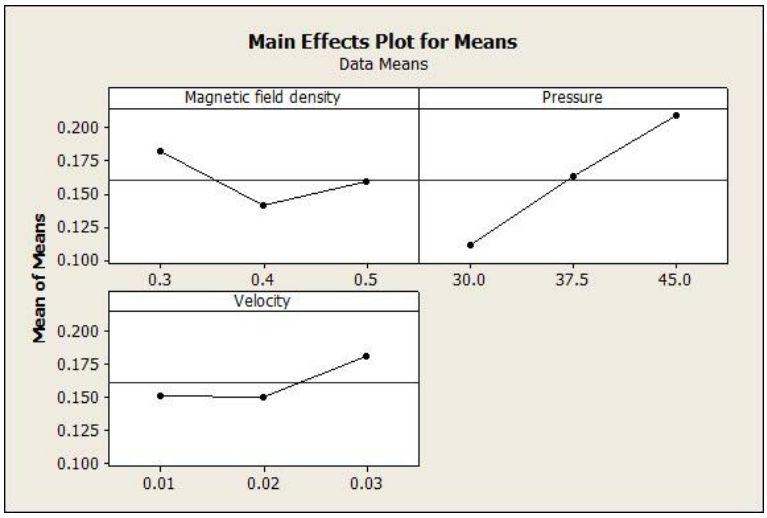

For the Means plot the higher values will give the optimum input parameters for the requirement consideration. So from the plot it can be said that the optimum paramaters for radial stress is 0.3T magnetic field density, 45 bar pressure and 0.03 m/sec velocity.

5.2.3 Indentation Depth

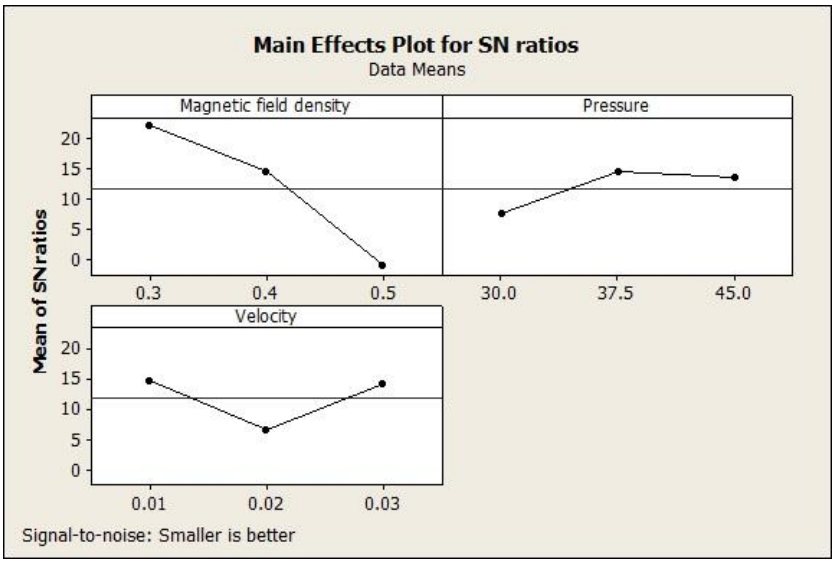

Considering the nano level finishing low indentation depth will be justified. So low value of indentation depth is required. That is why here lower is better criteria is taken. Now it is known that for the above criteria higher values of SN Ratio will give the optimum input parameters. So from the plot it can be said that the optimum paramaters for indentation depth are 0.3T magnetic field density, 37.5 bar pressure and 0.01 m/sec velocity.

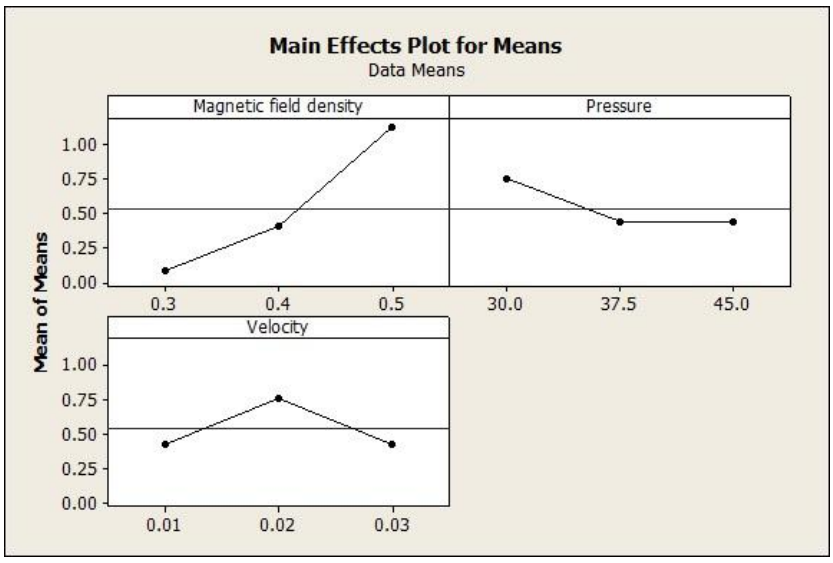

For the Means plot the higher values will give the optimum input parameters for the requirement consideration. So from the plot it can be said that the optimum paramaters for indentation depth is 0.3T magnetic field density, 37.5 bar pressure and 0.01 m/sec velocity.

Chapter 6 Conclusion

Based on the theoretical investigationobtainable from this study, subsequent conclusions have been developed

- From the CFD analysis it is validated with the theoretical model that shearing is happening during finishing, when applied shear force applied on the abrasive particle is more than the workpiece material's resisting force due to the strength of the material and it is the main cause of material removal.
- From the results obtained from the CFD analysis it can be concluded that the model predicts nano level finishing and model data is validated with available experimental results.
- When no magnetic effect is applied CIPs don't get that required bonding force corresponding to that the normal force is less which is required to indent the abrasive particle. So surface roughness achieved is less but material removal will occur as shear force is greater than reaction force.
- It is concluded that for optimizing the finishing process it is required that the value of axial stress and indentation depth should be low and value of radial stress should be high. The conclusions from the optimization made are following:
    - The optimum process parameters for minimizing axial stress are 0.3T magnetic density, 45 bar inlet pressure and 0.01 m/sec inlet velocity.
    - The optimum process parameters for maximizing radial stress are 0.3T magnetic density, 45 bar inlet pressure and 0.03 m/sec inlet velocity.
    - The optimum process parameters for minimizing indentation depth are 0.3T magnetic density, 37.5 bar inlet pressure and 0.01 m/sec inlet velocity.

REFERENCES

1. L.J. Rhoades, Abrasive flow machining, Manufacturing EngineeringNovember (1988) 75–78.
2. W.I. Kordonski, S.D. Jacobs, “Magnetorheological finishing”, Int. J. Mod. Phys. B 10 (23–24) (1996) 2837–2848.
3. S. Jha, V.K. Jain, Design and development of the magnetorheological abrasive flow finishing process, International Journal of Machine Tools & Manufacture 44 (2004) 1019–1029
4. T. Shinmura, K. Takazawa, E. Hatano, Study of magneticabrasive finishing, Annals of CIRP 39 (1) (1990) 325–328.
5. Y. Tani, K. Kawata, Development of high-efficient fine finishingprocess using magnetic fluid, Annals of CIRP 33 (1) (1984)217–220.
6. W.I. Kordonski, Golini Don, “Magnetorheological Suspension- Based High Precision Finishing Technology (MRF)”, Int. J. Mat. Sci. and Structures, Vol. 9, August 1998
7. Rosenweig, R.E., 1966. Fluid magnetic buoyancy. AIAA Journal 4 (10), 1751.
8. Tani, Y., Kawata, K., 1984. Development of high-efficient fine finishing process usingmagnetic fluid. Annals of CIRP 33, 217–220.
9. J. Rabinow, The magnetic fluid clutch, AIEE Transactions 67(1948) 1308.
10. M. Jolly, J. David Carlson, B.C. Munoz, A model of the behaviourof magnetorheological materials, Smart Material & Structure5 (1996) 607–614.
11. J.M. Sun, R. Tao, Viscosity of a one-component polarizablefluid, Physical Review E 52 (1) (1995) 813–818, July.
12. J.M. Ginder, L.C. Davis, Shear stresses in magnetorheologicalfluids: role of magnetic saturation, Applied Physics Letter 65(26) (1994) 3410–3412.

13. J.D. Carlson, D.M. Catanzarite, K.A. Clair, Commercial magnetorheologicalfluid devices, International Journal of ModernPhysics B 10 (23,24) (1996) 2857–2865.

14. J.D. Kim, M.S. Choi, Simulation for the prediction of surface accuracy in magnetic abrasive machining, Journal of Material Processing Technology 53 (1995) 630–642.

15. Jain, V.K.; Jayswal, S.C.; Dixit, P.M. Modeling and simulation of surface roughness in magnetic abrasive finishing using non-uniform surface profiles. Materials and Manufacturing Processes 2007, 22 (2), 256–270..

16. S.C. Jayswal, V.K. Jain, P.M. Dixit, Modeling and simulation of magnetic abrasive finishing process, International Journal of Advanced Manufacturing Technology 26 (2005) 477–490

17. Das M, Jain V. K and Ghoshdastidar P.S Computational fluid dynamics simulation and experimental investigations into the magnetic-field-assisted nano-finishing process (2012).

18. C.R. Beverly, R.I. Tanner, Numerical analysis of three-dimensional Bingham plastic flow, Journal of Non-Newtonian Fluid Mechanics 42 (1992) 85–115.

19. P.S. Ghoshdastidar, Computer Simulation of Flow and Heat Transfer, Tata McGraw-Hill, New Delhi, 1998.

20. A.W. Stradling, The physics of open gradient dry magnetic separation, Int. Journal of Mineral Processing 39 (1993) 1–18.

21. Das M., Jain V K, and Ghoshdastidar P.S, Analysis of magnetorheological abrasive flow Finishing (MRAFF) process, Int. J. of AdvancedManufacturing Technology, p613-621. 2008

22. R.K. Jain, V.K. Jain, P.M. Dixit, Modeling of material removal and surface roughness in abrasive flow machining process, Int. Journal of Machine Tools & Manufacture 39 (1999) 1903–1923.

23. W. Kordonski, D. Golini, Progress update in magnetorheologicalfinishing, International Journal of Modern Physics B 13 (14–16) (1999) 2205–2212.

24. V.K. Jain, Magnetic field assisted abrasive based micro-/nano-finishing, Journal of Materials Processing Technology209 (2009) 6022–6038